Wen *et al. Geo-Engineering (2017) 8:28*
https://doi.org/10.1186/s40703-017-0066-7

International Journal of Geo-Engineering

ORIGINAL RESEARCH Open Access

Numerical study of plastic response of urban underground rock tunnel subjected to earthquake

Kai Wen*, Hideki Shimada, Takashi Sasaoka and Zhiyi Zhang

*Correspondence:
wenkaicumt@hotmail.com
Laboratory of Rock Engineering and Mining Machinery, Department of Earth Resources Engineering, Kyushu University, Fukuoka 819-0395, Japan

Abstract

Underground facilities play an important role in infrastructure of modern society, especially some lifeline engineering, such as subway and railway tunnels, civil air-defense engineering and so on. As we know, the entire cognitive processes of seismic response of underground openings to earthquake is transforming from taking no account of earthquake load, primordially, to adopting the theory of free-field deformation, transitively, and the employing theory of dynamic design till now. However, so far, there are no established methods which can absolutely be employed for assessing and evaluating stability and induced plastic damage of tunnel surroundings ground during earthquakes. Based on a while building subway tunnel, this paper describes the propagation of seismic wave and seismic induced plastic damage of surrounding rock with a simple harmonic wave and a field recorded wave, which have the same dominate frequency. In addition, the specific energy density (SED) is introduced to represent the energy dissipation during ground shaking. Due to the recorded time-history wave, the response of feature points along tunnel and extension of plastic zone are analyzed with the different peak ground acceleration (PGA). Results illustrate that the upper tunnel cross section is more vulnerable than the lower part. Interestingly, when the PGA reaches 0.3 and 0.4 time of gravity acceleration, the seismic response of tunnel behaves almost the same.

Keywords: Seismic response, Plastic, Urban underground, Rock tunnel, Earthquake

Introduction

Because of the ever-increasing populations of large cities, the need for high capacity of transportation and storage has led to an increasing use of underground facilities, such as subway and railway tunnels, underground pipelines, civil air-defense engineering, sewage and water transport and so on [8]. In seismic active areas, underground tunnels are generally thought to be less susceptible to the earthquake damage compared to aboveground structures due to its strong seismic-resistance by nature [7, 10, 19, 20, 22]. There is a popular idea that the major reason for the reduction in underground damage is the lower levels of shaking at depth comparing with surface motions [19]. Even the current design codes in the United States of American for the highway structures do not take the seismic loads in the transverse direction into consideration unless the structure crosses an active fault [1]. It is generally acknowledged that the constraints of the surrounding

rock can commendably prevent the damage of underground openings from the earthquake loads. However, the recent earthquakes showed that underground structures are also vulnerable to seismic damage when subjected to earthquakes [4, 13], including the 1995 Kobe, Japan earthquake, the 1999 Chi–Chi, Taiwan, earthquake, the 1999 Kocaeli, Turkey earthquake and the 2008 Wenchuan, China earthquake [8].

In the seismic active regions, the support system must be designed to bear the static overburden loads of the surrounding rock as well as to accommodate additional deformations triggered by the seismic-induced ground shaking. The earthquake-induced ground deformations, along with the static earth and rock pressure, will cause the deformation of the surrounding rock and further development of plastic circle, which may bring about the pressure increasing around the support system and even the failure of support systems and collapse of underground openings.

As a matter of fact, the earthquake-induced inertia force of underground structures can be relatively small [9], even smaller than the inertia force of the surrounding ground. Based on the soil-structure interaction analysis of Samata et al. [18], it was indicated that the seismic response of underground structure is mainly governed by the ground displacement during earthquakes, which proves that it is the dynamic response of surrounding ground determining the dynamic response of underground structures. Therefore, it is very important to make clear of the response of surrounding rock when subjected to earthquake loads. However, the damage survey of tunnels subjected to earthquakes is still underway and the research of damage mechanism is still undergoing [3, 4] and should be further studied [22]. Up to now, there are no established approach which can be employed for assessing and evaluating tunnel stability during earthquakes, and the design specifications for earthquake protection in tunneling are lacking [23].

Comparatively speaking, the seismic response research of surface and underground structures themselves, such as liners, are much further than that of underground surrounding rock and soils. Analysis made by Wang [21], Penzien [16] and Pitilakis and Tsinidis [17] of the seismic response of underground structures, such as axial and curvature deformation, and ovaling or racking deformations, shows that the most critical deformation occurring within a tunnel lining during a seismic event is the racking of the cross-section.

The purpose of this paper is to further understand the surrounding plastic deformation and develop a reasonable and consistent seismic design methodology for underground transportation tunnels which would also be applicable to other underground structures. Therefore, in order to optimize design, we present a numerical modeling of these problems by using FLAC3D software. Regardless of the liners and soil-structure interaction, we primarily focus on the damage and extension of plastic zone of shallow tunnel surrounding rock, including quantitative analysis—response to a sinusoidal waveform and qualitative analysis—response to a recorded waveform.

Response to sinusoidal shear waves

Free-field deformation

Generally, the peak ground acceleration (PGA), peak ground velocity (PGV), peak ground displacement (PGD), response spectra and duration are mainly used to describe the intensity of earthquake ground motion. However, it is an extremely complicated

problem to describe the free-field ground behavior rigorously even without the consideration of ground-structure interaction. Therefore, for practical purposes, Newmark [14] proposed a simplified approach, based on the theory of wave propagation in homogeneous, isotropic and elastic media, in which the ground strains were calculated by assuming a harmonic wave traveling at an angle of incidence. Figure 1 shows the free-field ground deformations along a tunnel axis due to a sinusoidal shear wave with a wavelength, L, a displacement amplitude, D, and an angle of incidence, θ [12]. The shear distortion of ground caused by vertically propagation shear waves is probably the most critical and predominate type of seismic ground motions in many underground openings. Therefore, in this paper, we just take the sinusoidal wave as the vertical input seismic loading at the bottom boundary.

Numerical analysis of sinusoidal wave load

Problem definition

The dynamic analysis in FLAC3D is based on the explicit finite difference scheme to solve the full equations of motion, using lumped grid point masses derived from the real density of surrounding zones [11]. There are two main conditions contained in the program: (1) quiet boundary; and (2) free boundary. For the seismic loading, the time-history of velocity and acceleration cannot apply along the quiet boundary. In this section, we take the simplest mode of wave, the sinusoidal wave, showing in Fig. 2, as the input motion load of this problem, and then try to illustrate the dynamic response of surrounding ground to the earthquake load, theoretically.

The model that has been analyzed consists of homogeneous, isotropic and elasto-plastic Mohr–Coulomb rock materials, and the mechanical properties of surrounding rock are given in Table 1. Material damping was introduced by Rayleigh damping which is defined as follows [6]:

$$\xi_i = \frac{\alpha_R}{2\omega_i} + \frac{\beta_R \omega_i}{2} \tag{1}$$

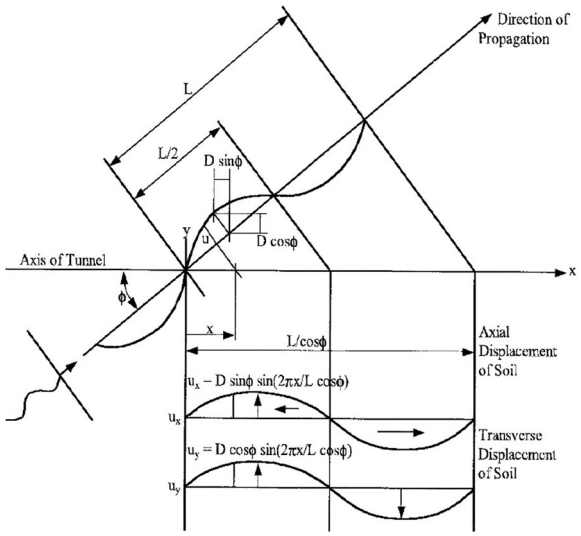

Fig. 1 Simple harmonic wave and tunnel [21]

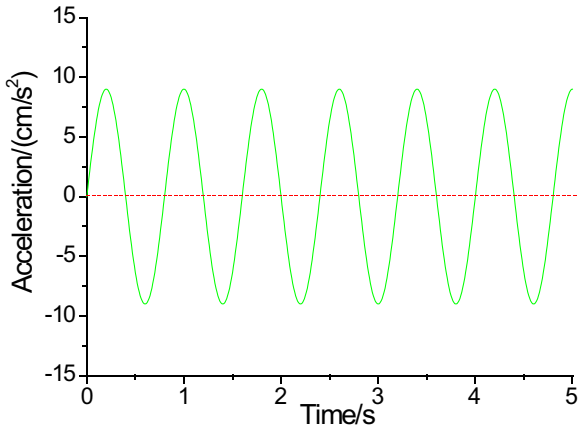

Fig. 2 Input of sinusoidal waveform

Table 1 Mechanical properties of rock

Density (kg/m^3)	Bulk modulus (MPa)	Shear modulus (MPa)	Friction	Cohesion MPa	Tension strength (MPa)	Damping
2500	4.0e8	2.3e8	30	2.2e4	1.5e7	0.05

where ξ_i and ω_i is the damping ratio and the circular frequency, respectively at mode i, α_R and β_R are Rayleigh damping coefficients proportional to the mass and stiffness. For the analyses described in this paper, only stiffness proportional damping was used. Material damping of the dry used rock material was taken as 5% based on the resonant column tests conducted by Bolton and Wilson [5]. The value of the stiffness proportional damping coefficient β_R was obtained using this damping ratio.

The numerical model has a length of 60 m, a height of 60 m, a width of 5 m, with a tunnel of 6 m excavation diameter, just conforming to one step of excavation of the tunnel. An elastic-perfectly plastic constitutive model, with failure criterion defined by the Mohr–Coulomb envelope, was assigned to the surrounding rock. Boundaries around the model are set as the viscous absorbing boundary, and the bottom bedrock boundary is set as static boundary, serving as input boundary of the earthquake load and the dynamic input wave is applied as an acceleration record. The geometry modeling is showed in Figs 3, 4.

The simulation procedure of this problem is divided into three steps: (1) initial stress state simulation; (2) post-excavation stress equilibrium; (3) applying the seismic wave along the bottom boundary.

Specific energy density (SED)

As we know, strong earthquake ground motion is primarily caused by the generation of large-amplitude and short-period seismic waves at the earthquake source in the fault zone. However, in general, the properties of seismic waves on the stratums' surfaces can be affected by the effect of the propagation path from the source to the site and by local site dynamic response effects, because seismic waves are attenuated by the propagation

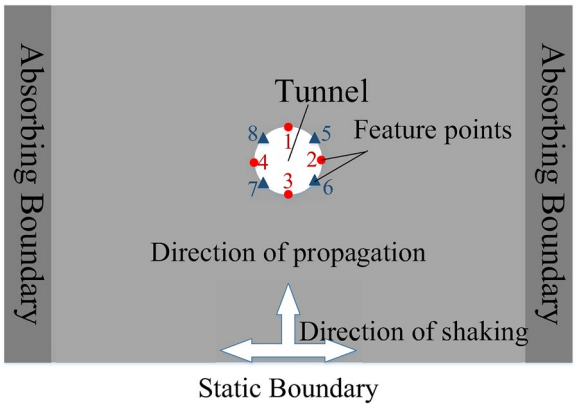

Fig. 3 Schematic diagram of numerical model (Points 1–8 are feature points)

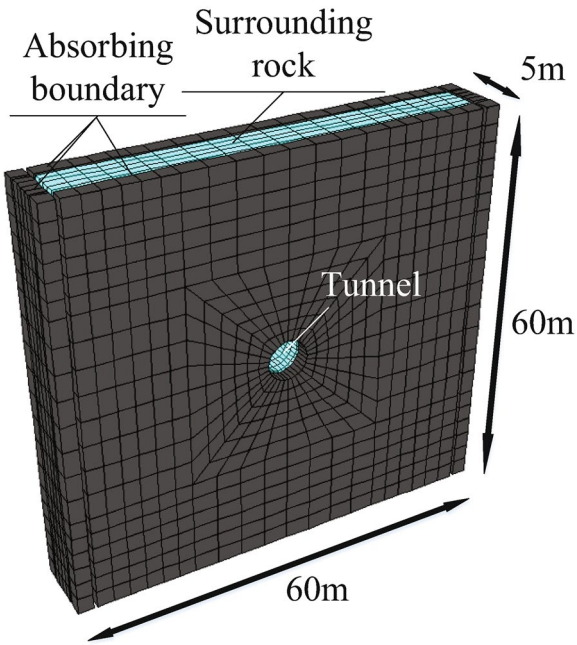

Fig. 4 Numerical model in FLAC3D

path, and may be attenuated or amplified by the site effects, which can cause the damage of surrounding ground of underground openings. Near-surface geological conditions plays a significant role on ground shaking, and earthquake damage can be accelerated by the ground motion amplification, due to sediments and soft rock near the ground surface [15]. Seismic wave propagates through rock and soil media and the earthquake energy dissipate gradually. The earthquake wave does not travel in a straight line, but the various curves with complicated forms after a bunch of reflections and transmissions. When seismic wave propagates vertically into varieties of interfaces, continuous reflections, transmissions and diffractions are generated, which causes the energy absorption by stratum material.

In this section, combining with the theory of energy absorption, the numerical experiments have been carried out accompanying with the sinusoidal wave input of 5 s. Meanwhile, we introduce the specific energy density (SED) to quantificationally estimate the damage of surrounding rock and evolution of plastic zone. SED is the square of velocity at any time integrated over the entire time range. The definition of SED is as follows:

$$\mathrm{SED} = \int_0^t [v(t)]^2 dt \tag{2}$$

where, $v(t)$ is the velocity.

Results

When the seismic wave is applied to the bottom boundary of the model as a shear stress wave loading, the wave propagates upwards perpendicular to the bottom static boundary while horizontal displacements occur in the ground as the amplitude of the wave decays with distance.

Figure 5 shows the response acceleration of feature points 1 (in Fig. 3) during the seismic numerical model, comparing with the sinusoidal acceleration wave. We can see from the graph that the original sinusoidal wave is smoothing, however, the response acceleration wave is unsmoothing, mingled with many ripples. This is because the reflections and transmissions of the seismic wave at the free boundaries and excavation boundary. Through the Fast Fourier Transform (FFT), Fig. 6 gives the results of spectrum analysis of response and sinusoidal waves, which demonstrates many low-frequency waves in the response spectrum.

As defined in the last section, the specific energy density (SED) is calculated depending on the Eq. (2). Figure 7 demonstrates the SED results of response wave and original wave, in which the shaded area stands for the energy dissipation during the propagation of seismic waves. This is the results from the elasto-plasticity of rock materials, meanwhile, the existence of excavation boundary is one of the reason for this.

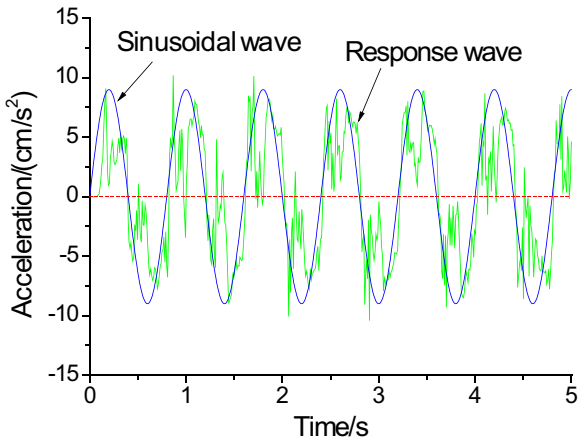

Fig. 5 Response acceleration time-history

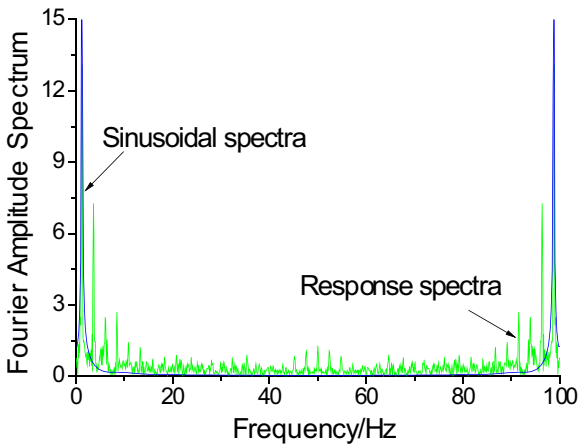

Fig. 6 Fourier amplitude spectra

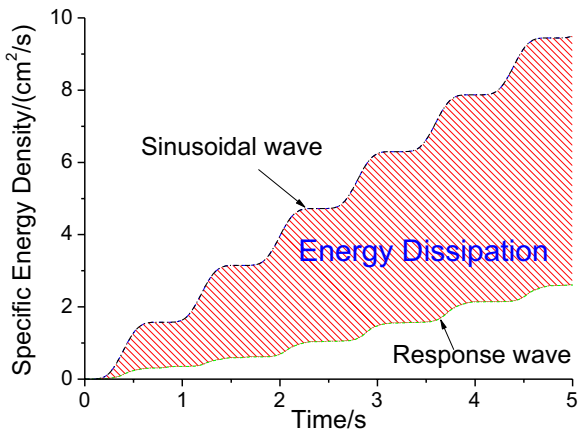

Fig. 7 Specific energy density

Response to recorded earthquake waves

Problem definition

In this section, the field recorded wave during earthquakes, Loma Prieta earthquake, Northern California, 1989, was used in the numerical model. Comparing with the sinusoidal wave, the recorded motion is a realistic motion and that it has a broad and rich frequency, which truly reflects the seismic response of tunnel surrounding to the earthquake. Before the seismic loading input, the processes of baseline correction and filtering should be performed to force both the final velocity and displacement to be zero [11]. The modeling geometry is the same with the last section, only differing in seismic loads input. In order to better understand the seismic response of under a particular intensity of ground motion, artificially amplifying and shrinking the waveforms to 0.1*g*, 0.2*g*, 0.3*g*, 0.4*g* and 0.5*g* ('g' stands for the gravidity acceleration), using the SeismoSignal software [2]. Figure 8 shows the surface recorded acceleration, velocity, displacement time-history during Loma Prieta earthquake, when the peak ground acceleration is set

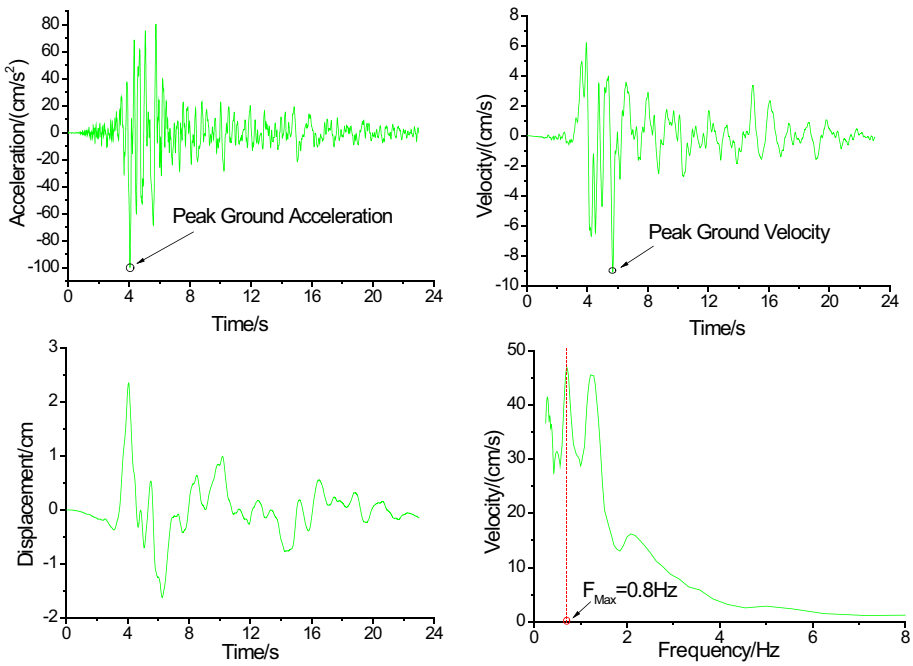

Fig. 8 Data time-history of Loma Prieta earthquake (PGA = 0.1*g*)

as 0.1*g*. From the velocity-frequency spectrum, we can see that predominant frequency of the recorded is 0.8 Hz, which is equal to the frequency of the sinusoidal wave.

Feature points analysis

Feature points

In the numerical simulation of this section, eight feature points are arranged along the excavation tunnel, showing in Fig. 3. Each feature point refers to a modeling element. During the simulation, the maximum principle stress is recorded of each monitoring element. And then, we extract the peak maximum principle stress (PMPS) of the maximum principle stress time-history, setting as the numerator, and extract the maximum principle stress of the same zone after static excavation, and setting as the denominator. In this way, we obtain the ratio of dynamic and static maximum principle stress, which can used to estimate the effect of various PGA of ground motion to underground openings. Figure 9 gives an example to obtain the peak maximum principle stress during the maximum principle stress time-history of zone ID = 297, and negative value indicates the compressive stress state.

Results

The ratio values of peak dynamic and static maximum principle stress represent the effect of earthquake to tunnel surrounding rock. Based on this, to understand the stress state of feature points during the earthquake is significantly important for the practical aseismic design and stability evaluation of underground openings. On the premise of this, it is very clear to know which parts of surrounding rock should be strengthen or which parts of liners should install the plastic hinges to avoid seismic damage.

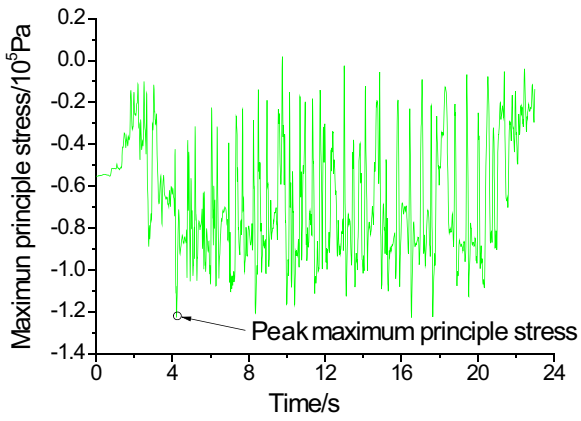

Fig. 9 Maximum principle stress time-history of zone ID = 297 (PGA = 0.1*g*)

Tables 2, 3 list the peak dynamic and static maximum principle stress of feature points 1–8, shoulder points 1–4 included in Table 2 and center points 5–8 included in Table 3.

Figures 10, 11 show the ratio of peak dynamic and static maximum principle stress of monitoring points 1–8. In the figures, we can see that almost all the ratio values are less than 1, which means that the compressive capacity of surrounding rock decreases because of the earthquake, except for the zone located in the uppers side of the tunnel section, such as vault and right shoulder positions. This is because the continuous rock arching effects of post-excavation under the vertical stress. However, the peak maximum principle stress of all the feature points increase gradually with the increasing of PGA after the sharp drop of post-excavation. Meanwhile, it can be seen from Fig. 10 that the stress relief induced by excavation causes the decreasing of static maximum principle stress in the tunnel invert (point 3), and the propagation of earthquake wave accelerates the stress relief.

Table 2 Peak maximum principle stress of points 1–4 (10^5 Pa)

PGA monitoring points	static	Loma wave				
		0.1*g*	**0.2*g***	**0.3*g***	**0.4*g***	**0.5*g***
Point 1 ID = 297	2.47	1.21	1.68	2.31	2.28	2.76
Point 2 ID = 785	6.0	1.48	2.5	4.23	4.02	4.88
Point 3 ID = 2265	4.7	2.23	2.45	2.89	2.94	3.98
Point 4 ID = 1441	5.55	1.48	1.53	2.12	1.98	2.28

Table 3 Peak maximum principle stress of points 5–8 (10^5 Pa)

PGA monitoring points	static	Loma wave				
		0.1*g*	**0.2*g***	**0.3*g***	**0.4*g***	**0.5*g***
Point 5 ID = 297	3.95	1.78	2.77	4.14	4.12	4.68
Point 6 ID = 785	8.80	0.75	1.04	1.61	1.42	1.70
Point 7 ID = 2265	6.23	2.84	2.95	3.3	3.43	4.26
Point 8 ID = 1441	3.67	0.07	0.11	0.71	0.5	0.58

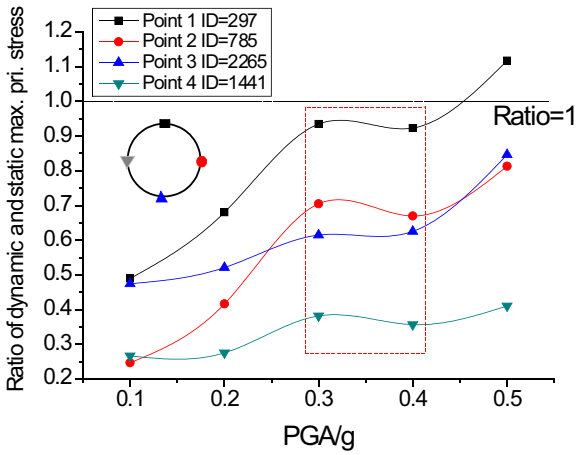

Fig. 10 Ratio of Max. Principle Stress of points 1–4

In Fig. 11, comparison analysis of shoulder points (points 5–8), the compressive capacity of surrounding rock near point 5 and 7 decrease more quickly than those of point 6 and 8 when subjected to earthquake. Obviously, asymmetrical influence subjected to seismic load on the arching positions exists, which proved that ovaling deformation of circle cross-section happens during the earthquake, which agrees well with the results of Hashash et al. [9], as red dotted ellipse in Fig. 11. Interestingly, when the PGA reaches 0.3*g* and 0.4*g*, the simulation results show that there is scarcely any difference of ratio value between them, for all the zones along the surrounding, showing in the red dotted rectangles. For this result, the properties of geological conditions and the characteristic of earthquakes waveform may play some roles in this result.

According to the results of dynamic simulation, based on the Eq. (2), the SED of point 1–8 can be calculated, described in Figs 12, 13. As shown in the figures, we can see that there is rarely SED generating before 4 s of time history, which is true with the acceleration and velocity time history. This also informs that we should pay more attentions

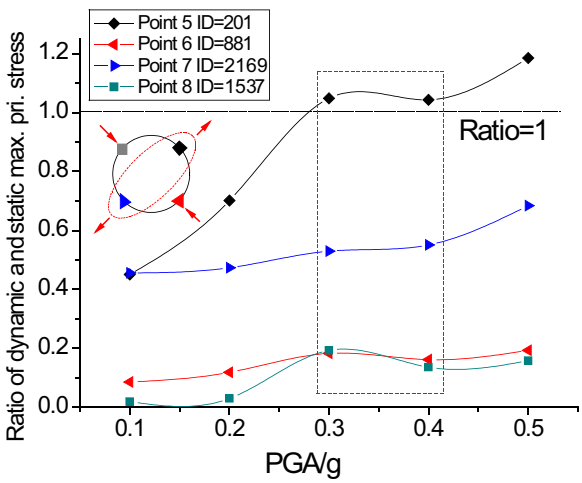

Fig. 11 Ratio of Max. Principle Stress of points 5–8

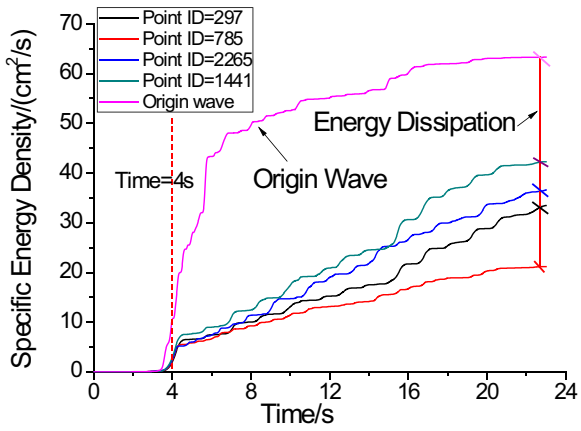

Fig. 12 SED of points 1–4

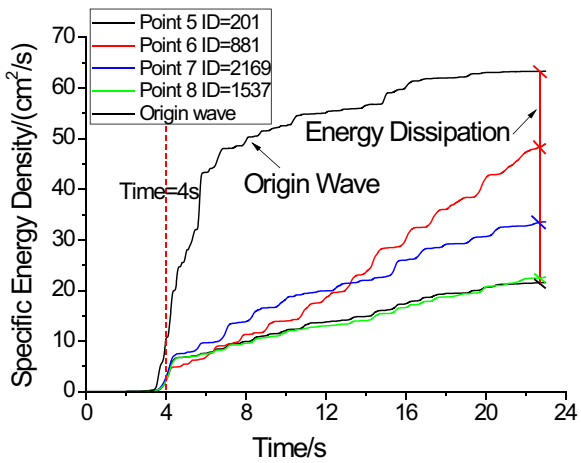

Fig. 13 SED of points 5–8

to the strong motion duration. The SED of origin wave is much higher than that of response wave of feature points around tunnel, because the energy dissipation happened continuously during the wave propagation though the elasto-plastic media. Obviously, both charts indicate that the points at upper cross-section of tunnel have larger wave energy dispersion than that of the points at lower part. That is to say, the plastic damage of upper section is also much more serious than the lower section, which means that more attentions are needed in the designing of supporting liner, especially joints and connecting interfaces, in the area with a high seismic level, comparing with the conventional method. However, due to the excavation and gravity of the overlying rock, upper section elements seem like have less damage, but this is not true.

Plastic extension analysis

Extension along with time-history

During the earthquake time-history, continuous vibration of ground will cause the unceasing damage of elasto-plastic geological material, reflecting in the extension of plastic circle along with the time-history. In the numerical simulation, the failure criterion is defined by the Mohr–Coulomb envelope, and the plastic state refers to the stress state reaches the yielding, not failure, thus we take the plastic zone size as a symbol of the seismic response grade, in which an isotropic material will fail, with any effect from the intermediate principal stress being neglected. From the acceleration time-history of PGA equaling to 0.1*g*, the acceleration reaches peak at 4 s, at which the plastic damage is most acute and extension of plastic zone size is largest. After the PGA, with the decreasing of wave density, the plastic zone size reduces, showing in the following Fig. 12.

Extension along with PGA

The extension of plasticity along with various PGA is shown in Figs 14, 15. We can take note that, with the increasing of PGA, the plastic zone size is raising continually in numerical model. In addition, the seismic-induced damage is mainly gathered around the surrounding of tunnel and areas near the surface. On the one hand, the dissipative

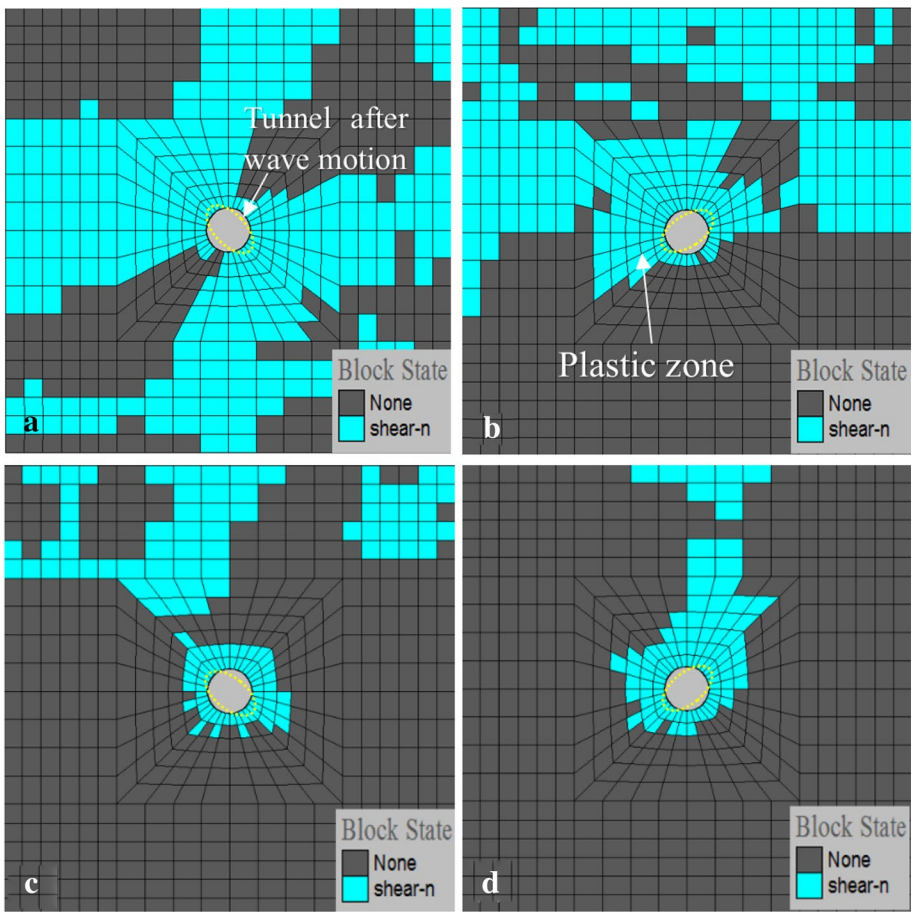

Fig. 14 Plastic zone size vs. time **a** 4 s, **b** 9 s, **c** 20 s, **d** 23 s

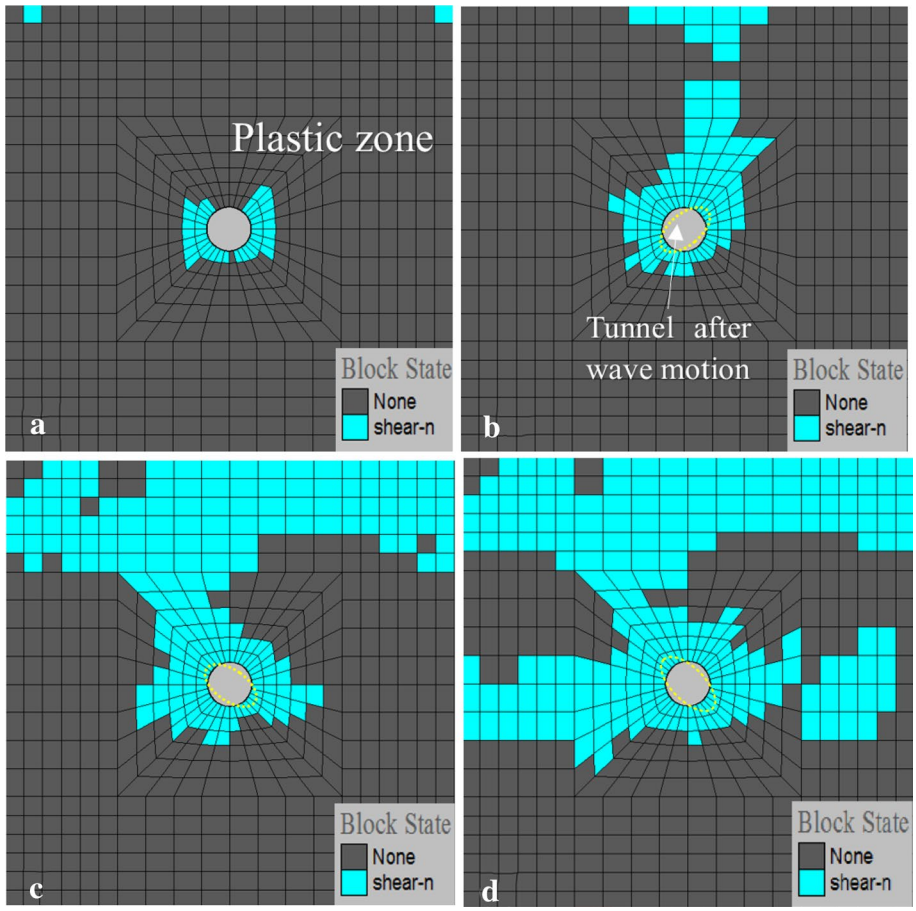

Fig. 15 Expansion of yielding zone vs. PGA. **a** Static, **b** PGA = 0.1*g*, **c** PGA = 0.3*g*, **d** PGA = 0.5*g*

energy of earthquake wave makes the stress-redistribution areas more vulnerable and lower bearing capability; on the other hand, seismic wave propagating at the regions near surface will be amplified and cause the maximum shaking, which will induce those areas into plastic state. From the unsymmetrical extension of plastic circles, we can see that seismic loading will result in the alternant diagonally distortion of tunnel section.

Discussions

This paper proposed a three-dimension numerical simulation modeling to study the dynamic response of tunnel surrounding rock under a sinusoidal wave and a field recorded earthquake waveform, respectively. Results have shown that seismic wave propagating in the Mohr–Coulomb rock material causes the additional damage of tunnel surrounding rock expect for the damage of static loads, and this is because the energy dissipation during wave propagation, which is the reason of the extension of plastic circle during earthquake.

1. For almost all the feature points along the tunnel, the ratio of dynamic and static maximum principle stress is less than 1, which means that compressive capacity of surrounding rock decreases subjected to the effect of earthquake, except for the zone

located in the upper section, vault and right shoulder position. This is because the continuous rock arching effects of post-excavation under the vertical stress.

2. However, the peak maximum principle stress of all the feature points increase gradually with the increasing of PGA after the drop of post-excavation. Meanwhile, obviously, asymmetrical transformation of tunnel section on the arching positions exists, which proved that ovaling deformation happens during the earthquake, agreeing well with the research of Hashash et al. [9].
3. Interestingly, when the PGA reaches 0.3 and 0.4 time of gravity acceleration, the seismic response of tunnel surrounding rock induced earthquake behaves nearly the same. Maybe, the properties of geological condition of field and characteristics of seismic waveform can lead to this result.
4. Meanwhile, based on the theory of energy dissipation, results show that upper part of tunnel cross-section has larger wave energy dispersion than the points at lower part, which means plastic damage of upper part is more serious than the lower part.
5. From the above, in the seismic active regions, the surrounding rock of tunnel should be strengthened, such as backfill-grouting, anchor bolt support and fiber reinforced concrete liner, especially the upper side of the tunnel section. Besides, in consideration of the ovaling deformation, the diagonal parts should set plastic hinges to improve ductility and to prevent distorting damage and failure.

Authors' contributions
KW mainly put forward ideas of this paper, and conducted the numerical simulation and data analysis, and finally wrote this paper. HS and TS proposed some good ideas to make this paper more valuable and helped to edit the manuscript. ZZ helped to improve the English. All authors read and approved the final manuscript.

Acknowledgements
The author wishes to thank China Scholarship Council (CSC). No. 201506420034.

Competing interests
The authors declare that they have no competing interests.

Consent for publication
Not applicable.

Ethical approval and consent to participate
Not applicable.

Publisher's Note

Received: 9 May 2016 Accepted: 7 December 2017
Published online: 14 December 2017

References

1. Aashto L (1998) LRFD bridge design specifications. American Association of State Highway and Transportation Officials, Washington, DC
2. Antoniou S, Pinho R, (2004) Software seismosignal. Version
3. Asakura T, (1997) Mountain tunnels performance in the 1995 Hyogoken-Nanbu earthquake. In: The 2nd international symposium on recent advances in exploration geophysics (RAEG 1997)
4. Asakura T, Shiba Y, Matsuoka S, Oya T, Yashiro K, (2000) Damage to mountain tunnels by earthquake and its mechanism. In: Proceedings-Japan Society of Civil Engineers, DOTOKU GAKKAI, 27–38
5. Bolton M, Wilson J (1990) Soil stiffness and damping. Cambridge Univ, Engineering Department, Cambridge
6. Cilingir U, Madabhushi SG (2011) A model study on the effects of input motion on the seismic behaviour of tunnels. Soil Dyn Earthq Eng 31:452–462
7. Dowding CH, Rozan A (1978) Damage to rock tunnels from earthquake shaking. J Geotech Eng Div 104:175–191
8. Hashash YM, Hook JJ, Schmidt B, John I, Yao C (2001) Seismic design and analysis of underground structures. Tunn Undergr Space Technol 16:247–293

9. Hashash YM, Park D, John I, Yao C (2005) Ovaling deformations of circular tunnels under seismic loading, an update on seismic design and analysis of underground structures. Tunn Undergr Space Technol 20:435–441
10. He W, Wu Z, Kojima Y, Asakura T (2009) Failure mechanism of deformed concrete tunnels subject to diagonally concentrated loads. Computer-Aided Civil Infrastruct Eng 24:416–431
11. Itasca F (2000) Fast Lagrangian analysis of continua. Itasca Consulting Group Inc., Minneapolis
12. Kuesel TR (1969) Earthquake design criteria for subways. J Struct Div 95(6):1213–1231
13. Lin M-L, Chung C-F, Jeng F-S, Yao T-C (2007) The deformation of overburden soil induced by thrust faulting and its impact on underground tunnels. Eng Geol 92:110–132
14. Newmark NM (1967) Problems in wave propagation in soil and rock, selected papers. In: Nathan M (ed) Newmark Civil Engineering Classics. ASCE, Reston, pp 703–722
15. Ohnaka M (2013) The physics of rock failure and earthquakes. Cambridge University Press, Cambridge
16. Penzien J (2000) Seismically induced racking of tunnel linings. Earthq Eng Struct Dyn 29:683–691
17. Pitilakis K, Tsinidis G, (2014) Performance and seismic design of underground structures. In: Earthquake geotechnical engineering design. Berlin: Springer, pp 279–340
18. Samata S, Ohuchi H, Matsuda T (1997) A study of the damage of subway structures during the 1995 Hanshin-Awaji earthquake. Cem Concr Compos 19:223–239
19. Sharma S, Judd WR (1991) Underground opening damage from earthquakes. Eng Geol 30:263–276
20. Towhata I (2008) Geotechnical earthquake engineering. Springer Science & Business Media, Berlin
21. Wang J-N (1993) Seismic design of tunnels: a simple state-of-the-art design approach. Parsons Brinckerhoff, New York
22. Wang W, Wang T, Su J, Lin C, Seng C, Huang T (2001) Assessment of damage in mountain tunnels due to the Taiwan Chi–Chi earthquake. Tunn Undergr Space Technol 16:133–150
23. Wang Z, Gao B, Jiang Y, Yuan S (2009) Investigation and assessment on mountain tunnels and geotechnical damage after the Wenchuan earthquake. Sci China Ser E Technol Sci 52:546–558